In Situ Synthesis and Properties of Epoxy Nanocomposites

Ludmila Bogdanova, Ludmila Kuzub, Emma Dzhavadjan, Evgenia Rabenok, Gennady Novikov, Anatoly D. Pomogailo*

Summary: silver-epoxy nanocomposite films based on diepoxide of Mn = 450, silver tetradecanoate and triethylamine were synthesized by *in situ* method. The mean diameter of AgNPs in nanocomposite films as defined by SEM technique has been found within the range of 15–20 nm. Ag NPs narrow size distribution was found independent on silver tetradecanoate concentration as shown by UV-vis spectroscopy analysis. Dielectric properties of silver-epoxy nanocomposite films were investigated also by Broadband dielectric spectroscopy technique.

Keywords: broadband dielectric spectroscopy; epoxy films; *in situ* synthesis; nanocomposite; silver nanoparticles

Introduction

Nanoparticles (NPs) as fillers in composites are more effective in comparison with large-scale particles. However NPs high surface energy makes them unstable due to selfaggregation phenomenon. The most perspective way to protect NPs is to use polymer-assisted fabrication of nanoparticles and nanocomposites.[1,2] A great number of publications had been devoted to the epoxy nanocomposites now.[3,4] Epoxy resin is one of perspective polymers to produce nanocomposites due to their unique properties such as high mechanical and dielectric properties, high adhesion, chemical resistance, etc.[5–7] On the other hand silver NPs have high optical, electrical, catalytic and bactericidal properties.[8] Besides silver NPs are very suitable objects for investigation of nanocomposite formation features because of surface plasmon resonance phenomenon.[9]

Nanocomposite production can follow two main routes: *in situ* and *ex situ* approach. In the first case, processes of polymer matrix synthesis and NPs generation from precursor are combined; while in the second approach polymer shell-coated NPs are dispersed within the polymer matrix *In situ* approach is generally preferred to *ex situ* procedure for technological purpose. Therefore *in situ* synthesis of silver-epoxy nanocomposite has both scientific and practical significance.

Last years some publications were devoted to this problem. *In situ* synthesis of silver-epoxy nanocomposites was achieved by simultaneous visible light photoinduced and cationic polymerization processes of Si- containing diepoxide and silverfluoroantimonate as NPs precursor. Ag NPs within epoxy matrix have the narrow size distribution between 15 and 20 nm.[10–12] Uniform dispersion of Ag NPs in epoxy matrix was prepared i*n situ* process by thermal decomposition of silver-imidazole complex as NPs precursor and following polymerization of diepoxide. The Ag NPs size was of around 11.6 nm.[13]

Synthesis and Characterization of Silver-Epoxy Nanocomposite Films

Nanocomposites as films of 100 μm thickness were synthesized by *in situ* method from DGEBA-based epoxy of $M_n = 450$ (ED), triethylamine (TEA, 5 wt. %.) and

Institute of Problems of Chemical Physics RAS, 142432 Chernogolovka, Russia
Fax: +74965227763; E-mail: bogda@icp.ac.ru

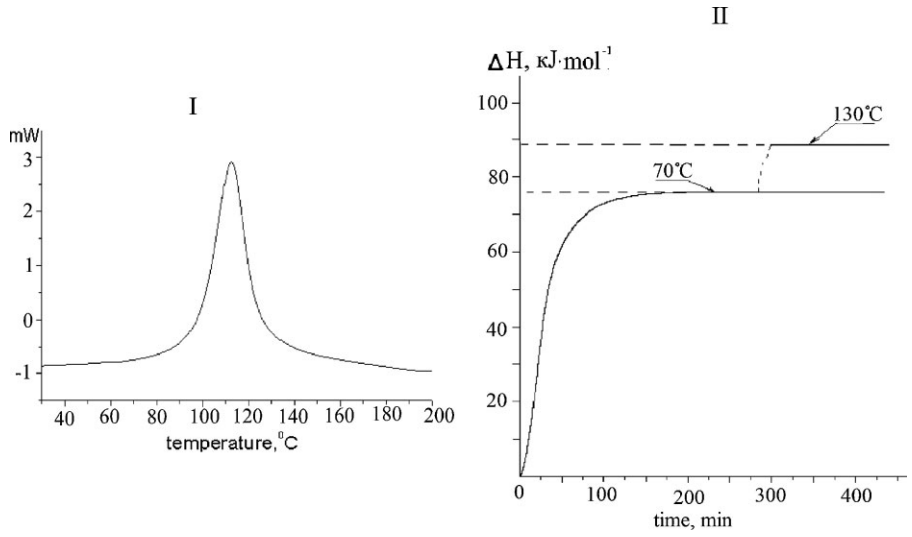

Figure 1.
DSC (I) and isothermic calorimetry of ED + 5% TEA (II).

silver tetradecanoate (AgMy, 0.05–0.56 wt. %.) as precursor of NPs. The reaction mixture was degassed to avoid bubbles. The correct degassing conditions were found experimentally. Then the reaction mixture was poured between two antitack agent treated glasses. The glasses were screwed together to prevent the reaction mixture to flow out. Then they were placed in hot oven to cure.

To determine the cure temperature regime the epoxy curing kinetics was studied by isothermic and differential scanning calorimetry methods. It was found by DSC technique that the curing heat was $\Delta H = 87\,kJ \cdot mol^{-1}$ (Figure 1).

The step by step temperature regime as 70 °C for 5 hours and 130 °C for 3 hours guaranteed a total curing heat of $\Delta H = 87\,kJ \cdot mol^{-1}$ and epoxy group conversion of about 0.95–0.98. A complete conversion of epoxy groups cannot be reached because of the inhibition effect at high conversions. The last is due not only to transition of the reaction into the region of diffusion control because of glass transition but also to chemical peculiarities of the reaction.[14,15]

In the curing process TEA acts as both reducing agent for silver tetradecanoate and curing catalyst for epoxy. These two reactions can be illustrated according to the following Scheme 1. First reaction of synthesis of monodispersed AgNPs with average diameter 4.4 ± 0.2 nm capped by long-chain alkyl carboxylates in TEA excess was proposed at first by M. Yamomoto et al.[16] (Scheme 1, I) The second reported reaction is catalytic reaction of epoxy curing under tertial amine. (Scheme 1, II) Kinetics, thermodynamics and mechanism of reactions of epoxy oligomers with amines was described in details by B. Rozenberg.[13]

I

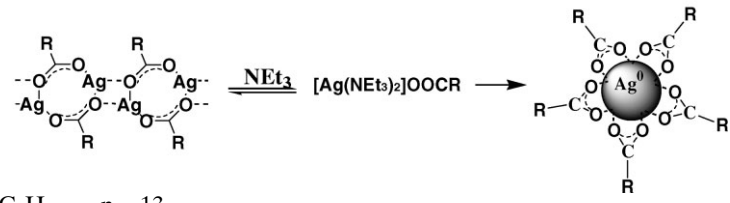

where $R = C_nH_{2n=1}$, $n = 13$

II

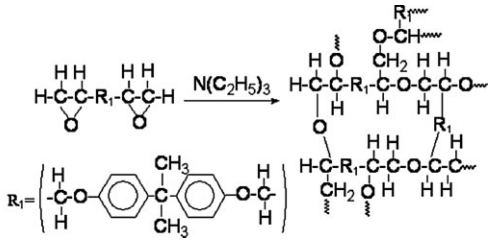

As a result of these two reactions the transparent yellow silver-epoxy nanocomposite films of 100 μm thickness were obtained. These films were characterized by UV-vis Spectroscopy, SEM, DSC and Broadband dielectric spectroscopy (BDS) methods. Figure 2 and Table 1 show UV-vis spectroscopy results of silver-epoxy nanocomposite films measurements. The main feature of Ag NPs absorbance spectra is intensive characteristic band in the region of 420–430 nm, so called Peak of Surface Plasmon Resonance (PSPR).[9]

The Peak intensity and position and the shape of spectra are dependent on many factors such as Ag NPs concentration, dispersion level, form, size and dielectric permittivity of medium around NPs. The increase of Ag NPs size shifts the Peak position to the long wave region of spectra. The increase of polydispersity level changes the symmetrical shape of spectra as far as broadening and disintegration of it.[8]

Table 1.
The UV-vis spectroscopy results of silver–epoxy nanocomposite films

C_{AgMy} $M \cdot 10^3$	PSPR[a] nm	half-width nm	A_{PSPR}	$C_{Ag\ NPS}$ $M \cdot 10^3$	$C_{Ag\ NPS}/C_{AgMy}$
5.3	427	65	0.31	3.1	0.6
8.9	421	47	0.61	6.1	0.7
11.9	419	49	0.96	9.6	1.0
19.9	420	50	2.28	22.8	1.1

[a)] Peak of Surface Plasmon Resonance.[b)] absorbance at PSPR.[c)] concentration, mol · l^{-1}.

The data of Figure 2 and Table 1 show the independence of PSPR position on initial AgMy concentration (except for $C_{Ag\ NPs} = 5.3 \cdot 10^{-3}$ M). Therefore NPs size does not change and does not depend on initial concentration of AgMy. The symmetric shape of spectra and spectra half-width is independent on AgMy concentration too. This is the argument to suppose the narrow size distribution of Ag NPs in silver-epoxy nanocomposite films.

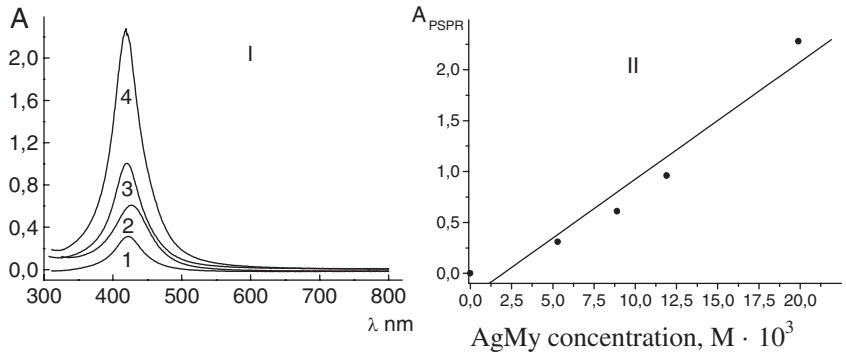

Figure 2.
UV-vis absorption spectra of Ag–epoxy nanocomposite films at different AgMy concentrations, $M \cdot 10^3$: 1–5.3, 2–8.9, 3–11.9, 4–19.9 (I) and $A_{PSPR} - C_{AgMy}$ dependence. (II).

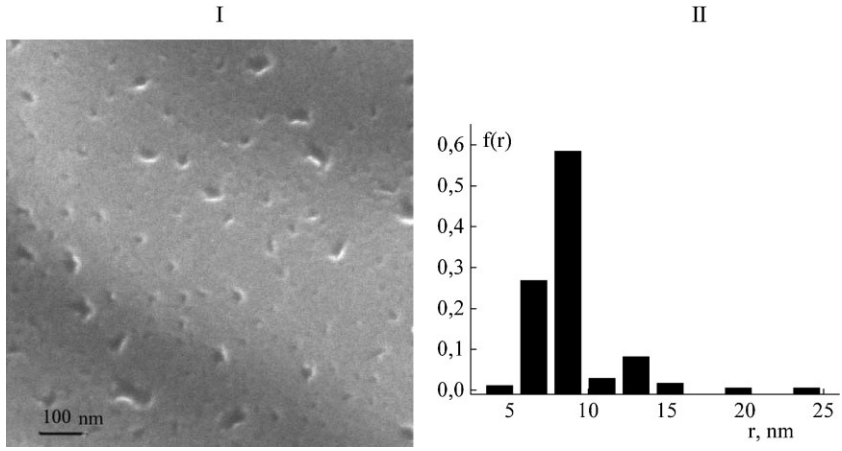

Figure 3.
SEM image of (ED + TEA + 0.05 wt. % AgMy) film (I); size distribution of Ag NPs calculated on the image area 1430 × 1430 nm (II).

The $A–C_{AgMy}$ dependence is linear. Since as the PSPR intensity depends on Ag NPs concentration, the last can be preliminary estimated using spectroscopic data. As follows from Buger-Lambert-Ber's law $A_{PSPR} = \sigma_{ext}$ C l, where A_{PSPR} is absorbance at PSPR, $\sigma_{ext}(l \cdot mol^{-1} \cdot cm^{-1})$ is extinction, $C(mol \cdot l^{-1})$ is Ag NPs concentration at PSPR and l(cm) is the thickness of nanocomposite film. PSPR is the Peak of Surface Plasmon Resonance. The correctness of calculation is defined by σ_{ext} value. The last depends on nanoparticle form and size and dielectric permittivity of medium around NPs. For example $\sigma_{ext} = (1 \div 3) \cdot 10^4$ $(l \cdot mol^{-1} \cdot cm^{-1})$ for Ag NPs in water solution. The data of Table 1 were calculated under assumption $\sigma_{ext} = 1 \times 10^4$ $(l \cdot mol^{-1} \cdot cm^{-1})$ as first approximation. The fact [Ag NPS/AgMy] > 1 demonstrates that $\sigma_{ext} > 1$. It is necessary to determine σ_{ext} value more exactly in the investigated system.

The yield of Ag NPs approaches to 1. But if initial AgMy concentration less then 10^{-2} M the reduction rate of Ag^+ to produce Ag NPs is less then the epoxy curing one and the yield of Ag NPs is decreased. Glass transition of epoxy matrix retards the reducing of AgMy.

The Ag NPs mean diameter within the range from 15 to 20 nm and size distribution as defined by SEM technique are shown in Figure 3.

Glass transition temperatures T_g of silver-epoxy nanocomposite films as defined by DSC method are independent on Ag NPs concentration substantially and were at the range of 110–115 °C. FTIR spectra of nanocomposites and epoxy network polymer are identical (Figure 4). Therefore the determinative factor in Ag NPs stabilization belong to the glass network structure of epoxy matrix. As follows from Figure 4 there is no band of epoxy group (911 cm^{-1}) in the case of ED + TEA (2) and ED + TEA + 0.29% AgMy (3) films. This is the evidence of complete curing process.

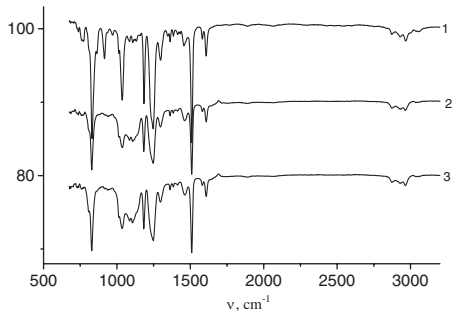

Figure 4.
FTIR-spectra of ED (1), (ED + TEA) film (2), (ED + TEA + 0.29 wt.% AgMy) film (3).

Broadband Dielectric Spectroscopy Measurements

All samples were investigated by using a broadband dielectric spectroscopy (Novocontrol Technologies GmbH & Co. KG, Germany) at the frequency range of $10^{-2} \div 10^{5}$ Hz and temperature within the range from $-140\,^{\circ}C$ to $+180\,^{\circ}C$. The temperature-frequency dependence of complex dielectric permittivity $\varepsilon^* = \varepsilon' - j\varepsilon''$ and specific electrical conductivity $\sigma^* = \sigma' + j\sigma''$ (where ε' and ε'' denote real and imaging part of complex dielectric permittivity, σ' and σ'' denote real and imaging part of complex specific electrical conductivity, $j = \sqrt{-1}$) of epoxy-silver nanocomposite films at different concentrations of Ag NPs were measured and analyzed.

The clear–cut plateau at low frequency reported by all tested samples which extend to higher frequency as the temperature increases is suitably related to the free charge transport. The conductivity values σ'', in the plateau region, corresponds to the direct current (dc) conductivity σ_{dc} and its dependency with temperature deviates considerably from Arrhenius behavior pointing out the significant contribution to cooperative effects for free charge carries transport mechanism. According to Vogel – Fulcher – Tammann, the dc conductivity can be fitted with following equation:

$$\sigma_{dc} = \sigma_{dc0}\ \exp\{-DT_0/(T - T_0)\}$$

to identify respectively, σ_{dc0}, D, and T_0 as fitting parameters (Figure 5). These two later parameters are respectively the Vogel temperature $T_{0,}$ which defines the dipole glass transition temperature, and strength parameter D, characterizing the deviation from Arrhenius linear behavior.

By using the D parameter values at different concentration of Ag NPs the glass transition temperature $T_{g,}$ can be analyzed according to the following relationship:

$$T_g = T_0(1 + 0.0255\,D)$$

The BDS measurements shows non-monotonically nanocomposite T_g and D

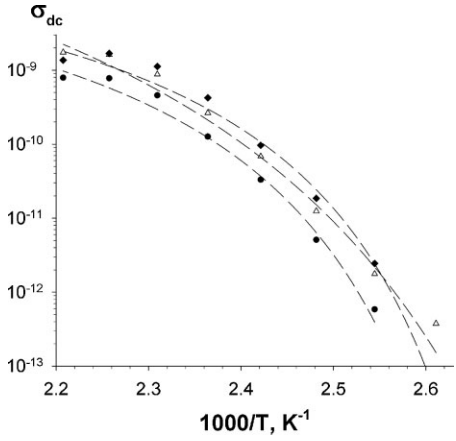

Figure 5.
Vogel-Tammann-Fulcher dependence for epoxy-silver films: ● = ED + TEA + $3.4 \cdot 10^{-3}$ M AgMy, ◆ = ED + TEA, Δ = ED + TEA + $19.9 \cdot 10^{-3}$ M AgMy. The lines are approximations by Vogel—Fulcher—Tammann (VFT) equation.

dependences on precursor concentration but at low precursor concentration ($<10^{-3}$ M) change of the T_g and D parameter is recorded. It was found that then and there the T_g increases accordingly to Ag NPs concentration within the range from 80 to 97 °C. (Figure 6).

The ''fragility concept'' (by means of D parameter) was introduced to take into

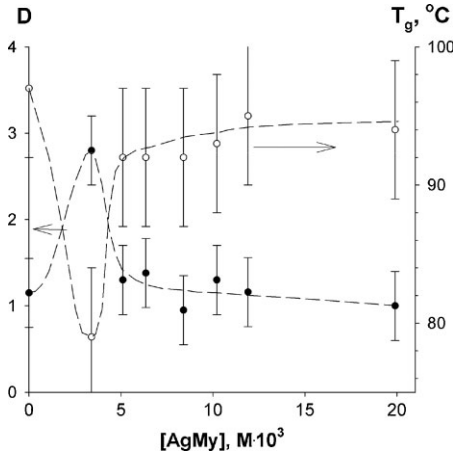

Figure 6.
The dependence of strength parameter D and glass transition temperature T_g on Ag NPs concentration: ● = D, ○ = T_g.

account the thermodynamic and kinetics features of glass transition. In fact, D value indicate the deviation of the temperature dependent functionality of $\sigma_{dc} = \varphi(1/T)$ from the Arrhenius linear dependency. In fact, lower D values are generally found for greater deviation from Arrhenius dependency,[17] as in the case of ''stable system'' such ionic glass ($D = 100$) while for ''unstable'' material, i.e. covalent glasses and polymer, significant lower values are encountered, i.e. 30 and 5–20, respectively.[18,19]

Conclusion

An *in situ* method is presented in order to produce epoxy nanocomposites using tertiary amine both as reducing agent for silver alkyl carboxylate and curing agent for epoxide. Two processes, i.e.–nucleation and growth of metall nanoparticles and epoxy curing - occur simultaneously with one of components taking part in both. Controlling of shape and size of metal nanoparticles represents a major issue for process optimization of epoxy nanocomposite formation. The viscosity increasing and glass transition in epoxy curing prevent NPs from aggregation and «freezing» the nanocomposite structure. Nanocomposite films are stable under storage for a long time due to glass state of epoxy network films. Spectroscopy reveals that the narrow size distribution of Ag NPS in epoxy nanocomposite films is not dependent on its concentration up to 10^{-2} M Ag NPs. DSC measurements show the slight nanocomposite Tg dependence on Ag NPs concentration at the range of 110–115 °C and thus Ag NPs does not change the epoxy matrix structure substantially within the range of 10^{-3}–10^{-2} M precursor concentration. The BDS investigation shows non-monotonically nanocomposite T_g and D dependences on precursor concentration. The T_g values defined by DSC and by BDS are not identical due to the different measurement technique.

Preliminary experiments show that proposed *in situ* synthesis of epoxy nanocomposites can be universal and usefull to reduce nanocomposite on basis of other metals such as Co, Ni, Cd, Pd and others.

[1] B. A. Rozenberg, R. Tenne, *Progr. Polym. Sci.* **2008**, *33*, 40–112.
[2] A. D. Pomogailo, V. N. Kestelman, *Metallopolymer nanocomposites*, Springer, Heidelberg **2005**, 563.
[3] S. Rana, R. Alagirusamy, M. Joski, *J. Reinforc. Plast. Compos.* **2009**, *8*, 461.
[4] V. I. Irzhak, *Usp. Khimii*, **2011**, *80*, 821–840.
[5] C. Lee, K. Neville, *Handbook of Epoxy Resins, Translation into Russian*, Moskva, Energiya **1973**, 415.
[6] B. A. Rozenberg, E. F. Oleinik, *Usp. Khimii*, **1984**, *53*, 273–289.
[7] V. I. Irzhak, B. A. Rozenberg, N. S. Enikolopyan, *Setchatye polimery: sintez, struktura, svoistva*, Moskva, Nauka **1979**, 248.
[8] Ya. Krutyakov, A. A. Kudrinsky, A. U. Olenin, G. V. Lisichkin, *Usp. Khimii*, **2008**, *3*, 242–269.
[9] U. Kreibig, M. Vollmer, *Optical Properties of Metal Cluster*, Springer, Berlin **1995**, 234.
[10] M. Sangermano, Y. Yagci, G. Rizza, *Macromolecules*, **2007**, *40*, 8827–8829.
[11] Y. Yagci, M. Sangermano, G. Rizza, *Polymer*, **2008**, *49*, 5195–5198.
[12] L. Vesco, M. Sangermano, R. Scarazzini, G. Kortaberria, J. Mondragen, *Macromolecular Chemistry and Physics*, **2010**, *211*, 1933–1939.
[13] H. Gao, L. Liu, Y. Luo, D. Jia, *Materials Letter*, **2011**, *65*, 3529–3532.
[14] B. A. Rozenberg, *Advances in Polymer Science*, **1986**, *75*, 113–165.
[15] L. Matejka, *Macromolecules*, **2000**, *33*, 3611–3619.
[16] M. Yamomoto, Y. Kashivagi, M. Nakamoto, *Langmuir*, **2006**, *22*, 8581–8586.
[17] N. A. Nikonorova, E. B. Barmatov, D. A. Pebalk, M. A. Barmatova, G. Dommguez-Espinosa, R. Diaz-Calleja, P. Pissis, *J. Phys. Chem. C*, **2007**, *111*, 8451–8458.
[18] C. A. Angell, *J. Non-Cryst. Solids*, **1991**, *13*, 131.
[19] R. Boehmer, K. L. Ngai, C. A. Angell, D. J. Plazek, *J. Chem. Phys.*, **1993**, *99*, 4201.

